Resonance-enhanced three-photon single ionization of Ne by ultrashort extreme-ultraviolet pulses

Resonance-enhanced three-photon single ionization of Ne by ultrashort extreme-ultraviolet pulses

Eiji Shigemasa[1,2,3]**, Mitsuru Nagasono**[3]**, Hiroshi Iwayama**[1,2,3]**, James R Harries**[3,4] **and Lisa Ishikawa (Okihara)**[1,5]

[1] UVSOR Facility, Institute for Molecular Science, Nishigonaka 38, Myodaiji-cho, Okazaki 444-8585, Japan
[2] SOKENDAI, Nishigonaka 38, Myodaiji-cho, Okazaki 444-8585, Japan
[3] RIKEN, SPring-8, Kouto 1-1-1, Sayo-cho, Hyogo 679-5148, Japan
[4] JAEA/SPring-8, Kouto 1-1-1, Sayo-cho, Hyogo 679-5148, Japan

E-mail: sigemasa@ims.ac.jp

Abstract
Time-resolved extreme-ultraviolet (EUV) fluorescence spectroscopy has been applied to study the multi-photon, single ionization of Ne irradiated by intense EUV-free-electron laser (FEL) pulses at a wavelength of 51 nm. A broad, intense peak at a wavelength of around 46 nm is observed, which is shorter than the incident FEL wavelength. The time dependence of the fluorescence reveals that the peak has two unresolved components, which we attribute to the decay of the excited ion states $Ne^+ 2s^{-1}(^2S)$ and $2p^{-2}(^3P^e)3s(^2P^e)$ at 46.0 and 44.6 nm. From the observed intensity ratios and fluorescence lifetimes we conclude that the $Ne^+ 2p^{-2}(^3P^e)3s(^2P^e)$ state is populated by two-photon resonance enhancement, via a $2p^43p^2$ doubly excited state of Ne.

(Some figures may appear in colour only in the online journal)

1. Introduction

With the advent of free-electron laser (FEL) facilities operating at wavelengths ranging from the extreme ultraviolet (EUV) to x-rays, we are undoubtedly entering a new age of photo-science. In the research field of atomic and molecular physics, nonlinear processes such as multi-photon absorption have become a major target to be investigated in the short wavelength region [1–9]. The modelling of nonlinear interactions of short-wavelength and short-pulse radiation with matter is essential for a wide range of basic and applied research, and thus there is a strong demand for understanding the physics behind the processes. The majority of the early work performed at FEL facilities made use of ion mass spectroscopy. Although the observed ion charge distributions provide general information on multi-photon processes, the detailed ionization pathways remain inaccessible. While electron spectroscopy can in principle be used to obtain more detail, only a few successful studies have been reported to date [7–9], due to the experimental difficulties involved. Reports to date include those on multi-photon ionization processes in Ar [7] and He [9], manifesting the power of the methodology.

Fluorescence spectroscopy can provide information on the energy levels of the excited neutral and ionic states involved in de-excitation processes following multi-photon ionization, which can be complementary to that obtained by photoelectron spectroscopy. The most remarkable advantage for fluorescence spectroscopy is that there are no space charge effects [10], which often cause serious problems for both photoelectron and ion mass spectroscopy. In addition, the recent successful observations of super-fluorescence from He atoms [11]

J. Phys. B: At. Mol. Opt. Phys. **46** (2013) 164020

E Shigemasa *et al*

and up-conversion fluorescence from Ar clusters [12] induced by the irradiation of EUV-FEL pulses clearly suggest the possibilities for controlling the chaotic nature of self-amplified spontaneous emission (SASE) FEL pulses by pumping gaseous, ionic or solid systems using pulses from one of the FEL sources. In the x-ray wavelength region, lasing has been observed on an inner-shell transition in Ne atoms [13], and suggested in molecules [14, 15].

In this work, we have studied EUV fluorescence in Ne following excitation with FEL pulses at a wavelength of 51 nm. Previous studies of the photoionization of neon using free-electron laser radiation have concentrated on much higher energy regions, where resonant processes in Ne^+ can occur following single-photon ionization [16]. A wavelength of 51 nm corresponds to excitation just above the Ne single-photon ionization threshold, and there are no excited states in this region. With intense pulses, however, it can be expected that multi-photon processes can occur, and we observed fluorescence at wavelengths near 46 nm. Fluorescence at this wavelength can be expected from the $2s^12p^5$ excited ionic state following either multi-photon absorption of the fundamental FEL radiation (51 nm) or single-photon absorption from the FEL harmonics (25.5 nm, 17 nm), but the details of the spectra cannot be explained by this process alone. By recording time-resolved spectra, we find evidence for resonance-enhanced (2+1) multi-photon ionization via a doubly excited state.

2. Experiment

The experiments were carried out at the EUV-FEL beamline at the SCSS test accelerator, which provided FEL pulses with a pulse energy of ~ 30 μJ and a pulse duration of ~ 30 fs [17]. The FEL radiation was linearly polarized in the horizontal direction, and the repetition rate was 30 Hz. A schematic diagram of the beamline can be found in [12, 18]. The EUV-FEL pulses are transported using a pair of flat mirrors in the accelerator tunnel to the experimental hall and then focused with a pair of elliptical and cylindrical mirrors [18]. The overall transmission of the beamline optics is estimated to be around 35% for the fundamental radiation. The pulse energy was monitored for each pulse using a photoion yield detector installed upstream of the focusing system. The focus size was about 12 μm in diameter. The pulse energy was controlled using an Ar gas attenuator upstream of the photoion yield detector. The intensity of the EUV pulses at the sample position was I $\sim 3 \times 10^{13}$ W cm^{-2}.

The focused FEL beam was introduced into a differentially pumped vacuum chamber. The gas nozzle had an aperture diameter of 500 μm. The effusive beam of Ne atoms flowed perpendicularly to the EUV-FEL radiation axis. EUV fluorescence emitted from the interaction region where the Ne atom beam crossed the FEL radiation was imaged through the entrance slit (width ~ 1 mm) of a flat-field grazing-incidence spectrometer (manufactured by Shinkukogaku Co., Ltd, Japan), which was set perpendicular to the EUV-FEL axis and parallel to the polarization vector of the FEL. The EUV fluorescence was dispersed by an aberration-corrected concave grating with a groove density of 400 1 mm^{-1} and focused

onto the detection plane. Time-resolved spectra were recorded using microchannel plates with a delay line anode (RoentDek, DLD-40). The resolving power $\lambda/\Delta\lambda$ of the present setup was estimated to be ~ 300, and the time resolution to be less than 0.2 ns. The wavelength scale of the spectrometer was calibrated by using monochromatized synchrotron radiation at BL5B of the UVSOR facility, Japan, in a separate measurement.

The contribution of higher harmonics to the total FEL intensity has previously been determined to be 1.1% at a fundamental wavelength of 51 nm [19]. In order to estimate the contribution in our spectra of the higher harmonics, we recorded spectra with the first-order (51 nm) intensity suppressed to 3% using the Ar gas attenuator. Since the photo-absorption cross sections of Ar are 36.8×10^{-18} cm^2 for the fundamental ($\lambda = 51$ nm), 2.9×10^{-18} cm^2 for the second harmonic ($\lambda = 25.5$ nm) and 1.2×10^{-18} cm^2 for the third harmonic ($\lambda = 17$ nm) [19–21], and it can be expected that any multi-photon processes will be severely suppressed by such a reduction in intensity, the spectra recorded under these conditions can be regarded as being purely due to single-photon absorption of the second and third harmonics. By subtracting these spectra from the spectra recorded with no attenuation, we obtain spectra only reflecting multi-photon absorption at 51 nm.

3. Results

Figures 1 and 2 show two-dimensional representations of fluorescence spectra recorded following single-photon absorption of the higher harmonics (figure 1) and multi-photon absorption of the fundamental at 51 nm (figure 2). The time axes correspond to the time differences between the incident FEL pulses and fluorescence detection. The simple EUV fluorescence spectra and time evolution of the fluorescence intensity are shown as (b) and (c), respectively, in each figure. The time 0 was set to the position of maximum fluorescence intensity. In the spectral region of interest in the present experiment (30–50 nm), the observed fluorescence is mainly due to the de-excitation processes of excited Ne^+ states to the ground ionic state Ne^+ $2p^{-1}(^2P^o)$. In figure 1(b), a single broad structure at a wavelength of ~ 46 nm is observed, which can be attributed to unresolved peaks due to the Ne^+ $2s^{-1}(^2S)$ $\rightarrow$ Ne^+ $2p^{-1}(^2P^o)$ and $2p^{-2}(^3P)3s(^2P)$ $\rightarrow$ Ne^+ $2p^{-1}(^2P^o)$ transitions. Weak peaks at wavelengths of around 33 nm, 36 nm and 41 nm can also be seen. These features can only be populated by single-photon absorption of the third harmonic at a wavelength of 17 nm, and can be associated with correlation satellites converging to double ionization thresholds. Kikas *et al* have identified the corresponding correlation satellites with $2p^{-2}nl$ configurations in their photoelectron spectrum, which was recorded at a photon energy h$\nu = 96$ eV (13 nm) [22]. The peak positions estimated from the satellites observed in [22] are shown as vertical lines with notations in figures 1(b) and 2(b), and are in good agreement with the observed structures in figure 1(b).

The peaks observed near a wavelength of 46 nm are very different for multi-photon and single-photon absorption. Only one island-like structure centred at 46.0 nm is seen in
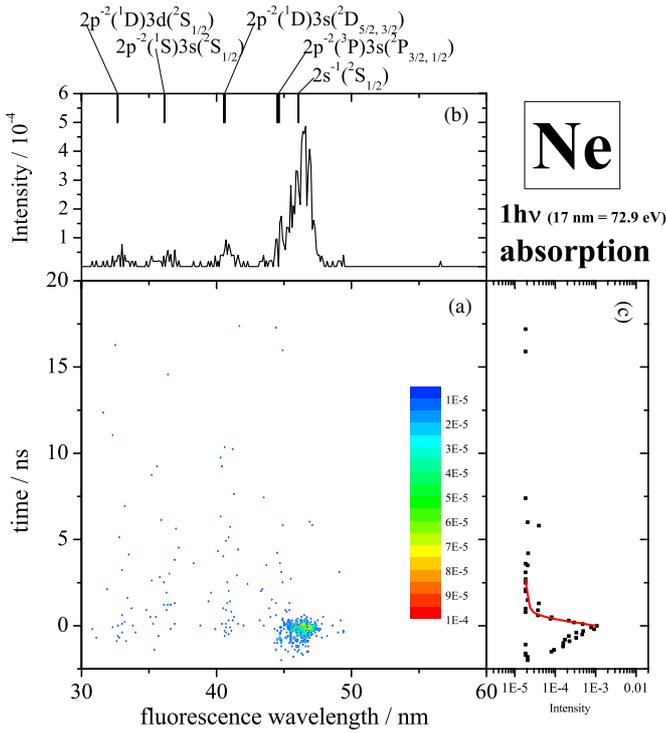
Figure 1. Time evolution of EUV fluorescence following single-photon absorption of harmonic FEL radiation (25.5 nm or 17 nm). The first-order photon intensity was suppressed to 3% using an Ar gas attenuator. (b) EUV fluorescence spectrum obtained by projecting the fluorescence intensity in the 2D map onto the horizontal axis. Some excited states of Ne$^+$ are shown. Note that only the 2s^{-1} state can be reached at 25.5 nm. (c) Time evolution of the fluorescence intensity obtained by projecting the fluorescence intensity in the 2D map onto the vertical axis. The red line shows a two-exponential fit to the data over the time range 0–2.8 ns.

Figure 2. (a) Time evolution of EUV fluorescence following multi-photon absorption at the fundamental FEL wavelength of 51 nm. The contribution of the higher harmonics (figure 1) has been subtracted. (b) EUV fluorescence spectrum obtained by projecting the fluorescence intensity in the 2D map onto the horizontal axis. (c) Time evolution of the fluorescence intensity obtained by projecting the fluorescence intensity in the 2D map onto the vertical axis. The red line shows a two-exponential fit to the data over the time range 0–2.8 ns.

figure 1(a), while a vertically long shape at a wavelength slightly shorter than 45 nm is also observed in figure 2(a). This suggests that there are additional processes contributing to the fluorescence observed for multi-photon absorption.

Figures 1(c) and 2(c) show the time dependence of the observed fluorescence. To determine the fluorescence lifetimes, the spectra have been fitted to an expression of the form

$$\ln(I(t)) = \ln\left(a_1 \times \exp\left(-t/\tau_1\right) + a_2 \times \exp(-t/\tau_2)\right) \quad (1)$$

where $I(t)$ is the fluorescence intensity, t is the detection time, a_i are the fluorescence intensities at $t = 0$, and τ_i are the fluorescence lifetimes. The fits were carried out on the time range of 0 to 2.8 ns, and we assume that the effects of the detector instrument function (responsible for the asymmetric profile for $t < 0$) can be ignored. The results of the fit are shown as solid red lines in the figures. The fit to the multi-photon data (figure 2(c)) revealed two components, with lifetimes of (1.5 ± 0.3) ns and (0.13 ± 0.03) ns. The fit to the single-photon data (figure 1(c)) revealed one component with a lifetime of (0.15 ± 0.02) ns, and a component with a lifetime of >7 ns, equivalent to a constant background for this dataset. From a comparison with the photo-electron spectroscopy results of [22], we can conclude that the short-lifetime components at a wavelength of 46 nm for both multi-photon
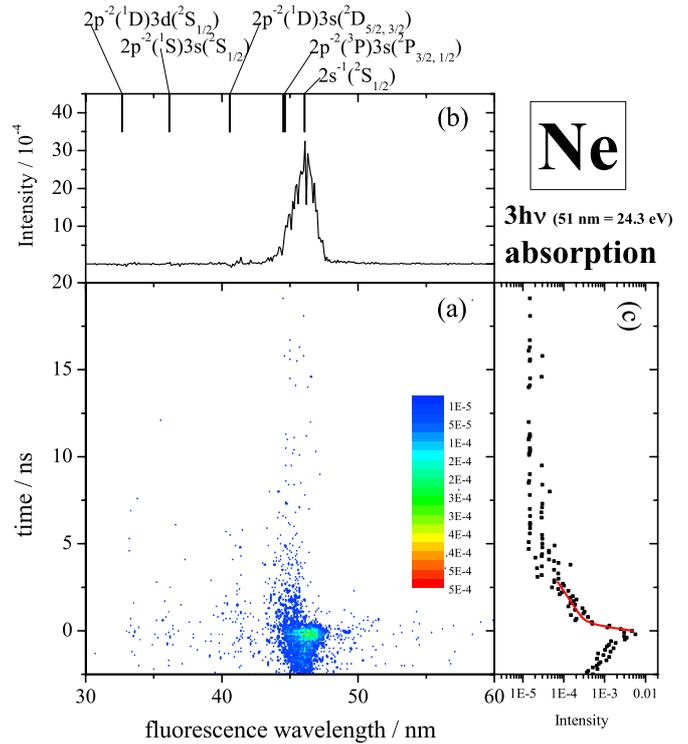
and single-photon absorption are due to fluorescence from the 2s^{-1}(^{2}S) state. The lifetime of this state has been determined to be around 0.15 ns [23], and published [24] and calculated [25, 26] theoretical results give similar values. The wavelength of the long-lifetime fluorescence ($\sim$44.6 nm) is consistent with the decay of the 2p^{-2}(^{3}P)3s(^{2}P) excited state to the ionic ground state [27, 28]. This state cannot be reached with two-photon absorption at 51 nm, even considering the bandwidth of the SASE pulses. To our knowledge, there have been no experimental or theoretical reports of the lifetime of this state, but atomic structure calculations suggest a lifetime of around 0.3 ns [25, 26]. We observe a much longer lifetime than this, suggesting that this transition is part of a cascade process, with the 2p^{4}3s state being populated through slower transitions at wavelengths beyond the sensitivity of our spectrometer.

The fits suggest that the ratios of the two decay routes 2s^{-1}(^{2}S): 2p^{-2}(^{3}P)3s(^{2}P) are around 1:1 for multi-photon excitation (figure 2(c)), and around 1:0 for single-photon excitation (figure 1(c)). This again is consistent with the results of [22], where a ratio of 1:0.003 was found for single-photon excitation at a wavelength of 13 nm. This result is striking, since while the absorbed energy is the same, the fluorescence intensity observed due to the decay of the 2p^{-2}(^{3}P)3s(^{2}P) state is at least 370 times as high for three-photon absorption than for

single-photon absorption (assuming a 1:0.003 ratio for single-photon absorption). Further, this enhancement is only seen for the $2p^{-2}(^3P)3s(^2P)$ state, and not, for example, for other $2p^{-2}(^3P)ns(^2P)$ states, which could be expected to have similar transition matrix elements. A similar result has previously been observed in He [9], where the enhancement of a particular excitation route was attributed to resonance enhancement of the two-photon absorption process. In neon, however, there are no states which can be reached with the absorption of a single photon of wavelength 51 nm (24.3 eV) [29]. The only possibility remaining is that the process is enhanced by a two-photon resonance, at a wavelength near 25.5 nm (48.6 eV). While the single-photon excitation of doubly excited states in this energy region has been studied with synchrotron radiation [30, 31], to our knowledge there have been no previous experimental studies of two-photon absorption to these states. Experimental and theoretical work on EUV or soft x-ray multi-photon absorption to date has concentrated on wavelength regions where excitation processes of Ne$^+$ can be studied [16, 32–34]. Some theoretical calculations also exist at wavelengths near the threshold for two-photon ionization of Ne [35, 36], but do not cover the current wavelength region or the possibility of two-photon doubly excited state resonant excitation. Considering the $^1S^e$ symmetry of the neon ground state and the selection rules for two-photon absorption, the $2p^{-2}(^3P)3p^2(^3P)(^1S^e)$ state appears to be a likely candidate. Langlois and Sichel [37, 38] give an energy of 48.6 eV for this state (with a claimed accuracy of 0.1 eV), which is well within the bandwidth of the SASE FEL pulses. The absorption of a third photon can remove one of the 3p electrons, to leave the excited ion state $2p^{-2}(^3P^e)3p(^2P^o)$. This state is known to decay to the ionic ground state through a cascade via the $2p^{-2}(^3P^e)3s(^2P^e)$ state, emitting UV fluorescence at a wavelength of around 330 nm and with a lifetime which has been reported experimentally to be 5.7 ns [39]. Theoretical calculations give values including 5.2 ns [40] and 4.4 ns [41]. The subsequent decay to the ground state is at a wavelength of 44.6 nm [27, 28]. It is this fluorescence which we detect, but the observed lifetime is dominated by the upper transition. While 5.7 ns is considerably longer than the 1.5 ns we estimate from our data, the estimated errors on both the theoretical and experimental values for the lifetime are quite large [41], and the count rate in our experiment quite low. While the count rate at short times is high enough to determine the short lifetime (0.15 ns) to a fair degree of confidence, longer lifetimes require increasingly higher cumulative counts. Further, we note that the doubly excited state we suggest for the two-photon resonance has never been observed experimentally (to our knowledge), and there may be other states in the vicinity within the bandwidth of the SASE pulses. Depending on which excited ion states are populated, the fluorescence we observe could be due to multiple cascade processes—again, a larger number of cumulated counts would be required to determine this. We can however conclude that our results qualitatively agree with the resonance enhancement of two-photon absorption, but that more detailed experiments are required to confirm the exact excitation and decay routes. The process we propose is summarized in figure 3. Note
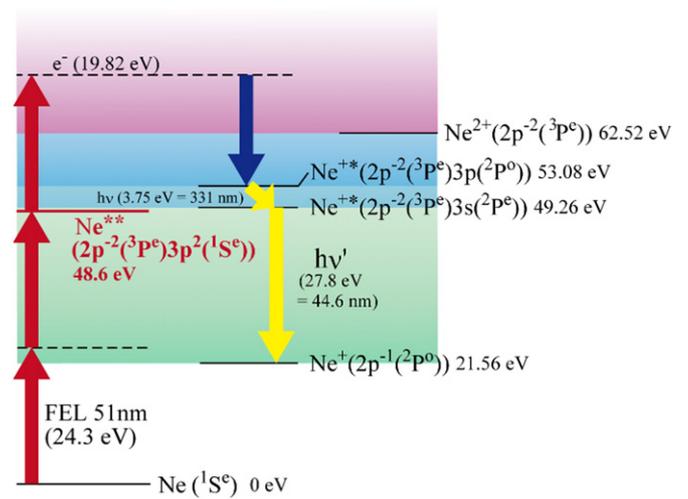

Figure 3. Schematic of the proposed two-photon resonant, three-photon ionization process. Two-photon absorption at 51 nm (red arrow) is resonantly enhanced by the Ne** $(2p^{-2}(^3P^e)3p^2(^1S^e))$ doubly excited state (horizontal red line). The absorption of an additional photon leads to ionization to the singly charged Ne^{+*} $(2p^{-2}(^3P^e)3p(^2P^o))$ state with the emission of a photoelectron (blue arrow). This state decays to the Ne^{+*} $(2p^{-2}(^3P^e)3s(^2P^e))$ state by emitting 331 nm fluorescence (short yellow arrow). Finally, EUV fluorescence at 44.6 nm is emitted, corresponding to the transition from the Ne^{+*} $(2p^{-2}(^3P^e)3s(^2P^e))$ state to the Ne$^+$ $(2p^{-1}(^2P^o))$ ground state (long yellow arrow).

that the occurrence of this process relies on the overlap with the 'spiky' profile of the SASE pulses overlapping strongly with the resonant state. This varies shot-by-shot, but the non-resonant parts of the spectrum still lead to non-resonantly enhanced multi-photon ionization leaving the ion in the excited $2s^12p^6$ state.

4. Summary

In summary, we have studied EUV fluorescence produced following multi-photon, single-ionization of neon, at a wavelength slightly above the threshold for ionization, but far from any single-photon excitation resonances in either Ne or Ne$^+$. Strong fluorescence was observed at around 46 nm which can only be attributed to multi-photon ionization to excited Ne$^+$ states. By studying the time dependence of the fluorescence, two separate processes were revealed, one of which can only be explained by a (2+1) three-photon resonant process involving the excitation of a neutral doubly excited state followed by the absorption of a further photon.

Acknowledgments

J. Phys. B: At. Mol. Opt. Phys. **46** (2013) 164020

E Shigemasa *et al*

References

[1] Young L *et al* 2010 *Nature* **466** 56–62
[2] Makris M G *et al* 2009 *Phys. Rev. Lett.* **102** 033002
[3] Wabnitz H *et al* 2005 *Phys. Rev. Lett.* **94** 023001
[4] Sorokin A A *et al* 2007 *Phys. Rev. Lett.* **99** 213002
[5] Rudenko A *et al* 2008 *Phys. Rev. Lett.* **101** 073003
[6] Meyer M *et al* 2010 *Phys. Rev. Lett.* **104** 213001
[7] Hikosaka Y *et al* 2010 *Phys. Rev. Lett.* **105** 133001
[8] Nagasono M *et al* 2007 *Phys. Rev.* A **75** 051406(R)
[9] Hishikawa A *et al* 2011 *Phys. Rev. Lett.* **107** 243003
[10] Posthumus J H 2004 *Rep. Prog. Phys.* **67** 623–65
[11] Nagasono M *et al* 2011 *Phys. Rev. Lett.* **107** 193603
[12] Iwayama H *et al* 2012 *Opt. Express* **20** 23174
[13] Rohringer N *et al* 2012 *Nature* **481** 488–91
[14] Kimberg V and Rohringer N 2013 *Phys. Rev. Lett.* **110** 043901
[15] Miao Q *et al* 2011 *Phys. Rev. Lett.* **109** 233905
[16] Martins M *et al* 2009 *Phys. Rev.* A **80** 023411
[17] Moshammer R *et al* 2011 *Opt. Express* **19** 21698–706
[18] Ohashi H *et al* 2011 *Nucl. Instrum. Methods Phys. Res.* A **649** 163–5
[19] Kato M *et al* 2009 *Nucl. Instrum. Methods Phys. Res.* A **612** 209
[20] Marr G V and West J B 1976 *At. Data Nucl. Data Tables* **18** 497–508
[21] Suzuki I H and Saito N 2005 *Radiat. Phys. Chem.* **73** 1–6
[22] Kikas A *et al* 1996 *J. Electron Spectrosc. Relat. Phenom.* **77** 241–66
[23] Curtis L J and Smith W H 1974 *Phys. Rev.* A **9** 1537–42
[24] Varsavsky C M 1961 *Astrophys. J. Suppl. Ser.* **6** 75
[25] Cowan R D 1981 *The Theory of Atomic Structure and Spectra* (Berkeley, CA: University of California Press)
[26] Gu M F 2008 *Can. J. Phys.* **86** 675–89
[27] Persson W 1971 *Phys. Scr.* **3** 133–55
[28] Kramida A E and Nave G 2006 *Eur. Phys. J.* D **39** 331–50
[29] Saloman E B and Sansonetti C J 2004 *J. Phys. Chem. Ref. Data* **33** 1113–58
[30] Lablanquie P *et al* 2000 *Phys. Rev. Lett.* **84** 431–4
[31] Schulz K, Domke M, Püttner R, Gutiérrez A, Kaindl G, Miecznik G and Greene C H 1996 *Phys. Rev.* A **54** 3095–112
[32] Hamonou L, Lysaght M A and Van der Hart H W 2010 *J. Phys. B: At. Mol. Phys.* **43** 045601
[33] Hamonou L and van der Hart H W 2008 *J. Phys. B: At. Mol. Opt. Phys.* **41** 121001
[34] Middleton D P W and Nikolopoulos L A A 2012 *J. Mod. Opt.* **59** 1650–63
[35] McKenna C and van der Hart H W 2004 *J. Phys. B: At. Mol. Opt. Phys.* **37** 457–70
[36] Lysaght M A, Van der Hart H W and Burke P G 2009 *Phys. Rev. A* **79** 053411
[37] Langlois J and Sichel J M 1980 *J. Phys. B: At. Mol. Phys.* **13** 881–9
[38] Langlois J and Sichel J M 1980 *J. Phys. B: At. Mol. Phys.* **13** 3109–16
[39] Bridges J M and Wiese W L 2007 *Phys. Rev.* A **76** 022513
[40] Zheng N W and Wang T 2003 *Spectrosc. Acta* B **58** 1319–24
[41] Santos J P, Costa A M, Madruga C, Parente F and Indelicato 2011 *Eur. Phys. J.* D **63** 89–96